https://doi.org/10.1016/j.buildenv.2017.03.011

Adopting 'Lift-up' Building Design to Improve the Surrounding Pedestrian-Level Wind Environment

K.T. Tse[a], Xuelin Zhang[a*], A. U. Weerasuriya[a], S.W. Li[b], K.C.S. Kwok[c], Cheuk Ming Mak[d] , Jianlei Niu[d,e]

[a]Department of Civil and Environmental Engineering, The Hong Kong University of Science and Technology, Clear Water Bay, Kowloon, Hong Kong.

[b]Division of Ocean Science and Technology, Graduate School at Shenzhen, Tsinghua University, Shenzhen, P. R. China

[c]Centre for Infrastructure Engineering, Western Sydney University, Australia

[d]Department of Building Services Engineering, The Hong Kong Polytechnic University Hunghom, Kowloon, Hong Kong.

[e]Faculty of Architecture, Design and Planning, The University of Sydney, Australia.

Corresponding author: Xuelin Zhang

E-mail address: xuelin.zhang@connect.ust.hk

Tel.: +852 55197725; fax: +852 23581534.

Mailing address: Department of Civil and Environmental Engineering, The Hong Kong University of Science and Technology, Clear Water Bay, Kowloon, Hong Kong

Abstract

Modern megacities are teeming with closely-spaced tall buildings, which limit air circulation at the pedestrian level. The resultant lack of air circulation creates poorly ventilated areas with accumulated air pollutants and thermal discomfort in the summer. To improve air circulation at the pedestrian level, buildings may be designed to have a 'lift-up' shape, in which the main structure is supported by a central core, columns or shear walls. However, a lack of knowledge on the influence of the 'lift-up' design on the surrounding wind environment limits the use of 'lift-up' buildings. This study aims to investigate the influence of 'lift-up' buildings and their dimensions on the pedestrian-level wind environments using wind tunnel tests. A parametric study was undertaken by using 9 'lift-up' building models with different core heights and widths. The results were compared with the surrounding wind environment of a control building with similar dimensions. The results reveal that the 'lift-up' core height is the most influential parameter and governs the area and magnitude of high and low wind speed zones around such buildings. Based on wind tunnel test results and a selected comfort criterion, appropriate core dimensions could be selected to have acceptable wind conditions near lift-up buildings.

Keywords: Building dimensions, 'Lift-up' building, 'Lift-up' core dimensions, Pedestrian-level wind environment, Wind tunnel test

1. Introduction

With the advent of light-weight construction materials and advanced structural forms, modern tall buildings are frequently designed with unusual shapes and complex forms. Some of these atypical shapes improve the aerodynamic performances of the buildings themselves and bring economic benefits to the developers. For example, the aerodynamic forces and wind excitations of tall buildings may be effectively minimised by tapered shapes and chamfered corners (Kawai, 1998; Tamura and Miyagi, 1999; Tse et al., 2009; Tanaka et al., 2012). In addition, certain building forms have proved useful in achieving acceptable wind conditions at the pedestrian level around buildings (Gandemer, 1975; Jamieson et al., 1992; Uematsu et al., 1992). In contrast to the influence of novel building forms on the aerodynamic behaviour of high-rise buildings, which has long been a topic for academic research and hence been thoroughly investigated, their influence on the pedestrian-level wind field has yet to be systematically studied. Considering the importance of the pedestrian-level wind fields in a tropical metropolis, it is necessary to analyse the impact of novel building forms on the pedestrian-level wind field in order to select appropriate building forms to produce acceptable pedestrian-level urban wind fields.

Wind nuisance in cities is typically caused by tall buildings, as they frequently produce unacceptable, even dangerous, windy conditions at the pedestrian level (Melbourne and Joubert, 1971; Murakami et al., 1986). Although high wind speeds are typically considered as the cause of pedestrian discomfort, wind-related environmental issues in cities such as Hong Kong, Tokyo, and New Delhi have switched from dangerously high wind speeds to undesirable low wind speeds (Tsang et al., 2012; Chetwittayachan et al., 2002; Goyal, 2002). Undesirable low wind speeds are a result of excessive sheltering by closely-spaced tall buildings, built in such a way to cope with the high land prices and scarcity of available lands in cities. Because developers do not want to lose usable space, there is a reluctance to reduce building dimensions

so as to provide more space for air to circulate. Newly developed building forms may be an alternative solution to improve pedestrian-level wind conditions in cities without sacrificing the useable space of a building. However, some common building forms used in cities impede air circulations by obstructing breezeways at the pedestrian level. Hong Kong is a classic example of a city where the use of inappropriate building forms has led to a deterioration of the urban wind environment. For example, closely-spaced tall buildings and bulk podium structures in Hong Kong substantially reduce wind penetration into the city and consequently generate undesirable low wind speeds at the pedestrian level (Yim et al., 2009; Ng, 2009; Tsang et al., 2012). Low wind speeds that allow air pollutants to remain near the ground also continue to exacerbate the air pollution in Hong Kong (Wang et al., 2006). Widespread stagnant air can be favourable to the spread of air-borne pathogens such the SARS virus (Severe Acute Respiratory Syndrome) and hence is a threat to the public health (Yu et al., 2004). Moreover, mean wind speeds smaller than 1.5 m s^{-1}, the minimum mean wind speed required by the Air Ventilation Assessment stipulated in Hong Kong, can cause outdoor thermal discomfort for pedestrians, especially in the hot summer months (Ng, 2009, Cheng et al., 2012).

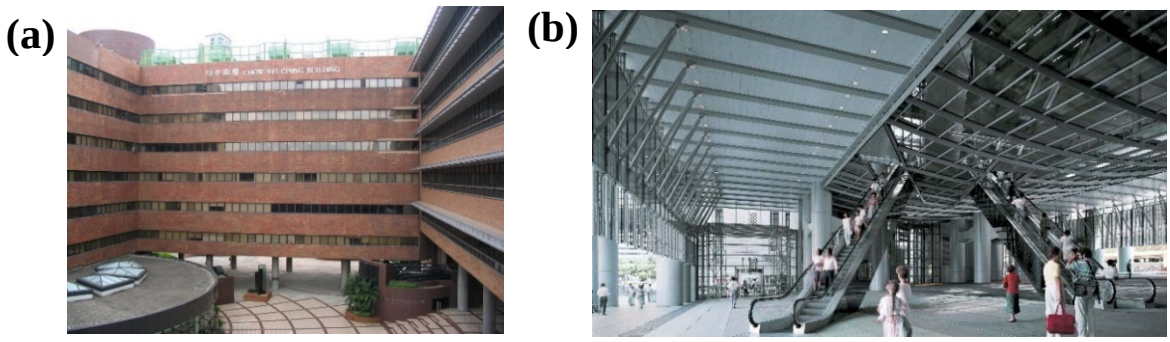

Figure 1. (a) A lift-up building in the Hong Kong Polytechnic University, Hong Kong, (b) 'lift-up' area of Hong Kong and Shanghai bank headquarter building, Hong Kong

The 'lift-up' building design is a potential solution for enhancing urban air ventilation in the city. The main structure of a 'lift-up' building is elevated from the ground by individually,

or a combination of, columns, shear walls, and a central core (Figure 1). The main structure elevated from the ground is known as 'lift-up' floors, and the ground area under the elevated main structure is referred to as the 'lift-up' area. The main benefit of the open space between the ground and the 'lift-up' floors is to minimise obstruction to wind flow at the ground level to enhance wind circulation at the pedestrian level (Hang and Li, 2010). In addition, the 'lift-up' area can be used as a recreational area, parking area, or a pathway to access other buildings or areas. The 'lift-up' design is, however, not widely adopted for buildings due to unacceptable or even dangerous high wind speeds found in the 'lift-up' area (Gandemar,1975; Beranek, 1984; Stathopoulos et al., 1992). These high wind speeds are a result of accelerated wind flows through narrowing openings, which connect positive and negative pressures on the windward and leeward sides of a building, respectively (Stathopoulos et al., 1992). However, the accelerated wind flows in the 'lift-up' areas may be favourable in achieving the minimum acceptable wind speeds in cities where undesirable low wind speeds prevail. In fact, Xia et al. (2015) have demonstrated that the addition of 'lift-up' floors to a single building, a building array, and building(s) with podium structure(s) can considerably increase the wind circulation around the building and is effective in achieving outdoor thermal comfort even under the prevailing low wind speed conditions in Hong Kong. However, Xia et al. (2015) employed a single core size thus no results are available to quantify the influence of the 'lift-up' core dimensions on the pedestrian-level wind field. This lack of understanding on influential parameters of 'lift-up' core dimensions prevents designers to adopt the 'lift-up' design to buildings in cities. Therefore, the present study aims to assess the influence of 'lift-up' core dimensions on the pedestrian-level wind environment, so as to be used to guide designers to adopt a 'lift-up' design for buildings to improve pedestrian-level wind conditions in a modern city such as Hong Kong. A series of wind tunnel tests were conducted using 9 isolated building models with different dimensions of central 'lift-up' core. Albeit being the simplest building

arrangement, isolated buildings are (1) able to generate less complex flow conditions than in a group of buildings, and (2) capable of producing all important flow features in the surrounding wind environment (Beranek, 1984; Hosker, 1985; Lam, 1992.) thus selected for the current study. On the other hand, a central core design would minimise the influence on wind conditions in the lift-up area, the main concern of this study, compared to rows of columns or shear walls at the perimeter of the building. In the wind tunnel tests, the wind speeds at the pedestrian level near lift-up buildings were measured and subsequently compared with wind speeds near a control building model (i.e., a building without the 'lift-up' design) with similar dimensions in order to identify flow features in pedestrian-level wind field modified by the 'lift-up' design.

The rest of the manuscript is organized as follows. After the introduction, section 2 presents the experimental setup of the wind tunnel tests, including details of the building models, measurement techniques, and approaching wind conditions. Section 3 discusses the results of the wind tunnel tests in three subsections; (1) the overall wind environment near the 'lift-up' building models, (2) the characteristics of the high and low wind speed zones around the 'lift-up' building models, and (3) the distribution of wind speeds in 'lift-up' areas. Concluding remarks are presented in section 4 in the form of a number of guidelines for designing 'lift-up' buildings in a modern city.

2. Experimental setup

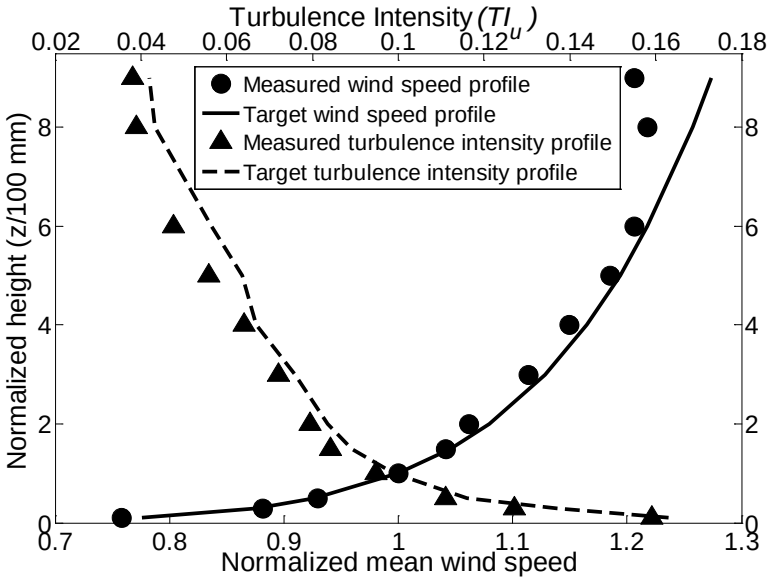

Figure 2. Normalized mean wind speed and turbulence intensity profiles at the centre of the turntable in the wind tunnel.

The wind tunnel tests described in this paper were conducted in the CPL Power Wind/Wave Tunnel Facility (WWTF) at the Hong Kong University of Science and Technology (HKUST), Hong Kong. The WWTF is a closed-return type boundary layer wind tunnel (BLWT) and has two parallel test sections named as "high speed" and "low speed" with different dimensions and operating wind speeds. The wind tunnel tests were carried out in the "low speed" section, which has a test section of 5 m x 4 m (width x height) and maximum operating wind speed of 10 m s^{-1}. The approaching wind speed and turbulence intensity profiles were simulated by arranging roughness elements and spires in the upstream of the flow development section, which is 41 metres long. Figure 2 displays the measured mean wind speed and turbulence intensity profiles at the centre of the turntable. The mean wind speed profile followed the power law wind profile model with an exponent of 0.11 (equation (1a)). The mean wind speed (U) and the longitudinal turbulence intensity (I_u), which is calculated as in equation (1b), measured at the 100 mm height at the centre of the turntable were 6.3 m s^{-1} and 9.5 %, respectively.

$$U(z) = U_{ref}\left(\frac{z}{z_{ref}}\right)^{0.11} \quad (1a)$$

$$I_u(z) = \frac{\sigma_u(z)}{\bar{u}(z)} \quad (1b)$$

In equation (1a), $U(z)$ is the longitudinal wind speed at height, z, and U_{ref} is the longitudinal wind speed at the reference height, z_{ref}. In equation (1b) $I_u(z)$ is the longitudinal turbulence intensity, $\bar{u}(z)$ is the longitudinal mean wind speed, and $\sigma_u(z)$ is the standard deviation of the longitudinal wind speed fluctuations.

The building models used in the study were designed based on a control building with full-scale dimensions of 120 m x 30 m x 20 m in height (*H*), width (*W*), and depth (*D*) respectively. All of the 'lift-up' buildings had a central core to elevate the 'lift-up' floors from the ground as shown in Figure 3. Table 1 shows full-scale dimensions of the 9 buildings modelled in this study. It is noted that the building models are different in terms of the dimensions of the core. More specifically, height (*h*), width (*w*) and depth (*d*) of the central core vary among the 9 buildings while the total height (*H*), width (*W*), and depth (*D*) of buildings remain constant. There were 3 core heights (i.e., 3 m, 6 m, and 9 m) and 3 core areas tested in the present study. The core area is expressed as the percentage of area covered by the core out of the plan area of the building at the ground level, termed as "area percentage" (*AP*). The selected core areas for this study had *AP* values of 9%, 25%, and 49%. All building models were manufactured using balsa wood to a length scale of 1:200.

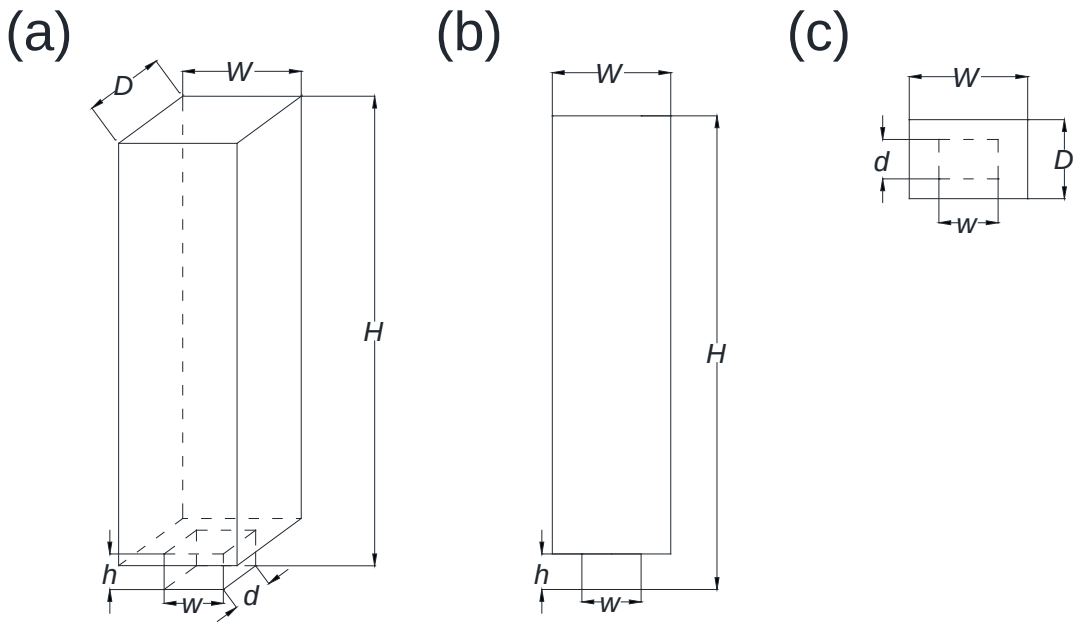

Figure 3. Schematic diagrams of a ‘lift-up’ building (a) 3-D view, (b) front view, and (c) plan view

Table 1. Full-scale dimensions of the 9 buildings

Model	Core dimensions			
	Core height (h) (m)	Core area		
		Width (w) (m)	Depth (d) (m)	Area percentage (AP) (%)
M1	3	9	6	9
M2	6			
M3	9			
M4	3	15	10	25
M5	6			
M6	9			
M7	3	21	14	49
M8	6			
M9	9			

The wind environments surrounding the building models at the pedestrian level were evaluated using mean wind speeds measured by Irwin sensors and Kanomax thermal anemometer system (Kanomax1560). The Irwin sensors used in the present study were

fabricated according to the 1:200 length scale with a 10mm height protruding tube. The protruding tube is to measure the wind speeds at the 10mm height, which is equal to 2m measurement height in the full scale. The mean wind speed (U) at the 10mm height was calculated from the Irwin sensors' raw measurements according to the method proposed by Irwin (1981), as

$$U = \alpha + \beta\sqrt{\Delta P} \tag{2}$$

In equation (2), $\sqrt{\Delta P}$ is the square root of the pressure difference between two holes on the Irwin sensor, and α and β are constants, which are determined from the curve fitting of mean wind speeds (U) measured by a hot-wire anemometer and $\sqrt{\Delta P}$ values. In the present study, α and β were estimated to be 0.15 and 1.72, respectively. Readers are suggested to refer studies of Irwin (1981), Wu and Stathopoulos (1994), and Tsang et al., (2012) for further information of Irwin sensor and its working principle.

The Kanomax1560 anemometer system is a multi-channel thermal anemometer system, which has multiple wind speed sensors and a data acquisition unit. The wind speed sensor is a spherical thermistor type omnidirectional sensor, which measures resultant mean wind speed a low sampling frequency at 10 Hz. Each sensor has a temperature compensator unit to correct any temperature effect on the measurements and is pre-calibrated with its own individual calibration curve. Its convenience in operating, and the ability to measure lower wind speeds are added advantages of Kanomax anemometer system being used in pedestrian-level wind tunnel tests.

Figure 4 displays the arrangement of 34 Kanomax anemometers and 186 Irwin sensors installed around the building model. The Irwin sensors were installed far-field of the measurement area while the Kanomax anemometers were installed in the vicinity of the building model including in the 'lift-up' area, where low wind speeds are anticipated. The two

types of sensors together covered a rectangular area spanning 375 mm in the upstream direction, 1425 mm in the downstream direction, and 600 mm in the lateral directions from the centre of the building model. As shown in Figure 4(a), the resolution of the Irwin sensor measurement grid was fine close to the building model and became coarse beyond a distance of 525 mm downstream of the building. The smallest spacing of the Irwin sensor measurement grid was 75 mm in the longitudinal direction and 100 mm in the lateral direction and satisfied the minimum separation distances proposed by Wu and Stathopoulos (1994). The minimum spacing of Kanomax anemometers was 30 mm in both the longitudinal and lateral directions. Both the Irwin sensors and Kanomax anemometers were operated via a common computer to record wind speeds data synchronously. The wind speed measurements at 10 mm height of both for Irwin sensors and Kanomax anemometers were recorded for 135 seconds at a sampling frequency of 400 Hz for the Irwin sensors and 10 Hz for the Kanomax anemometers.

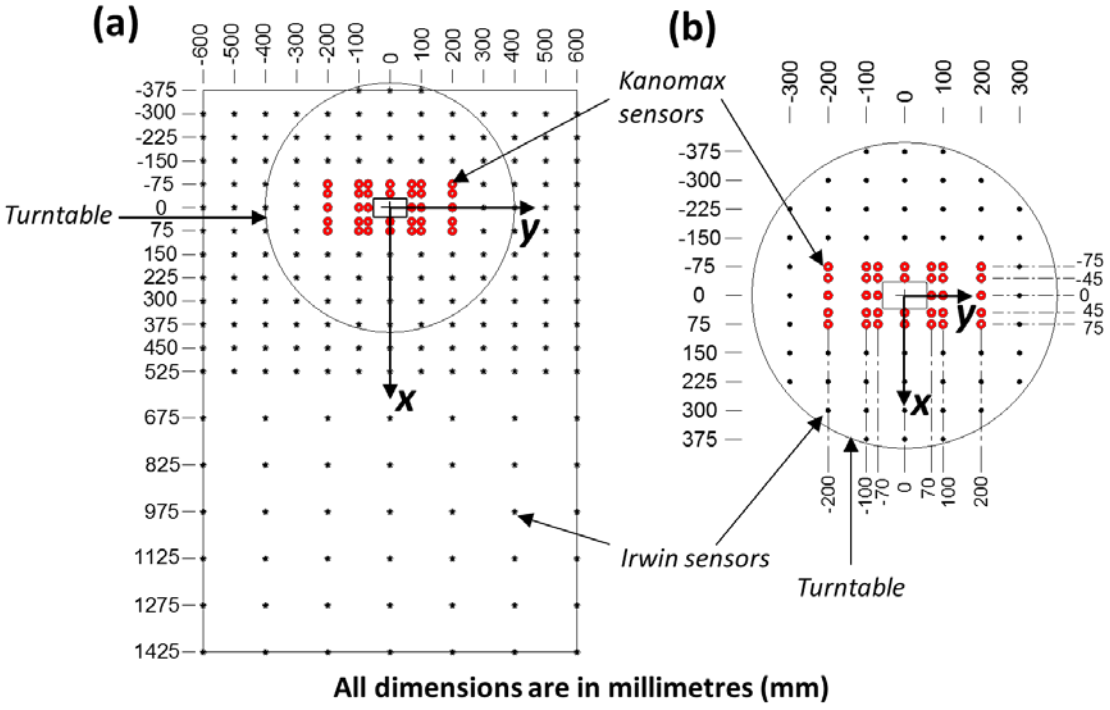

Figure 4. The sensor arrangement (a) in the whole measurement area, and (b) within the turntable (add the axis to figures)

3. Results and discussion

The normalized mean wind speed ratio (*K*) have been used effectively by previous researchers (Stathopoulos et al., 1992; Bottema, 1993; Tsang et al., 2012) to analyse the pedestrian-level wind environments. The advantages of the use of *K* value are its ability to eliminate the differences in wind speeds and turbulence intensities of incoming wind flows and only highlight the modifications occurred in the local wind environment near buildings. Moreover, by knowing the *K* values, designers can calculate corresponding wind speeds by using local meteorological wind speed data at a given location. For this study, *K* value is calculated by using the measured mean wind speeds at the 10mm height as expressed in equation (3).

$$K = \frac{\overline{U}_{10mm,x,y}}{\overline{U}_{10mm,ambient}} \tag{3}$$

where, $\overline{U}_{10mm,x,y}$ is the mean wind speed at the 10 mm height measured at a location (*x*, *y*), and $\overline{U}_{10mm,ambient}$ is the mean wind speed at the 10 mm height at the same location but without the building.

Figures 5 (a) and (b) display the distributions of the *K* values around a 'lift-up' building (i.e., model M5) and the control building (hereafter referred to as CB) respectively. The cubic interpolation method was used to plot the contours of *K* and all the distances were normalized with respect to the building depth (*D*). In figures, the red arrow on the upstream side of buildings points in the direction of the approaching wind.

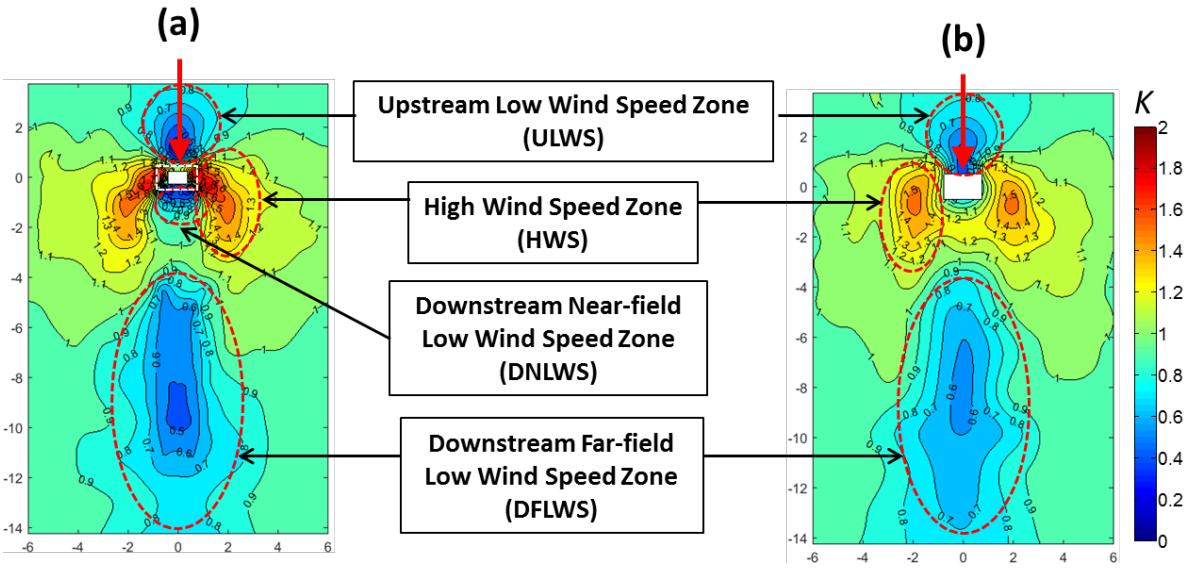

Figure 5. The distribution of the normalized mean wind speed ratio (*K*) in the surrounding of (a) model M5, (b) the control building (CB)

Owing to a number of flow modifications, the pedestrian-level wind environment surrounding the 'lift-up' building (model M5) is different from the wind field corresponding to the control building (CB), as shown in Figure 5. The most noticeable flow modification is found on the lateral sides of the 'lift-up' building where the corner streams (CS), which is also referred as the separation layers, are larger in size and higher in magnitude than of the CB. Moreover, the CS zones of model M5 are formed closer to the building in such a way that a portion of the corner streams is in the lift-up area, which is indicated by the dash rectangular box in Figure 5. The low wind speed (LWS) areas (marked by blue) corresponding to model M5 also display some noticeable differences from those found in the CB. Particularly, a distinct LWS area is formed next to the leeward side of model M5, whereas no downstream near-field low wind speed zone (the DNLWS zone) can be identified for the CB. The influence of the 'lift-up' floors gradually diminishes far downstream of the building as indicated by the formation of the downstream far-field low wind speed zone (the DFLWS zone) of model M5 at the same location as in the case of the CB. However, compared to the CB, model M5's

DFLWS zone has a larger area where K values are small ($K \leq 0.6$). Apparently, K values in the upstream direction of mode M5 (i.e., in the ULWS zone) are smaller than of the CB. Moreover, the ULWS zone is detached from model M5, whereas the ULWS zone is connected to the building in the CB

Figure 6 shows how the pedestrian-level wind fields around 'lift-up' buildings vary with height and area of the core. The dimensions of the 'lift-up' core supporting the 'lift-up' floors govern the magnitudes and sizes of the LWS and HWS zones near 'lift-up' buildings. Particularly, the HWS zones appearing on the lateral sides of the building display significant variations in size and magnitude with the core dimensions. For example, taller cores, such as in model M3, create larger HWS zones further away from the side walls of the 'lift-up' building. Shorter cores, on the contrary, produced smaller HWS zones closer to the building. Furthermore, the HWS zones, in some extreme cases, occupy a major portion of the 'lift-up' area, such as shown in Figure 6 corresponding to model M1. The 'lift-up' core height has marginal influence on the LWS zones in the upstream and downstream directions of the buildings as indicated by a slight increase of K values in the ULWS zone with the 'lift-up' core height. However, the location of the ULWS zone, whether it is attached to the building or not, is strongly dependent on the core height. As it can be seen in model M1, the shorter core (h=3 m) creates an attached ULWS zone, but in model M3, which has a taller core (h=9 m), produced a ULWS zone that is detached from the building. Compared to the 'lift-up' core height, the core area has some distinct influences on the LWS zones both in the upstream and downstream directions of the buildings including the formation of bigger DNLWS zones with smaller K values by larger core areas.

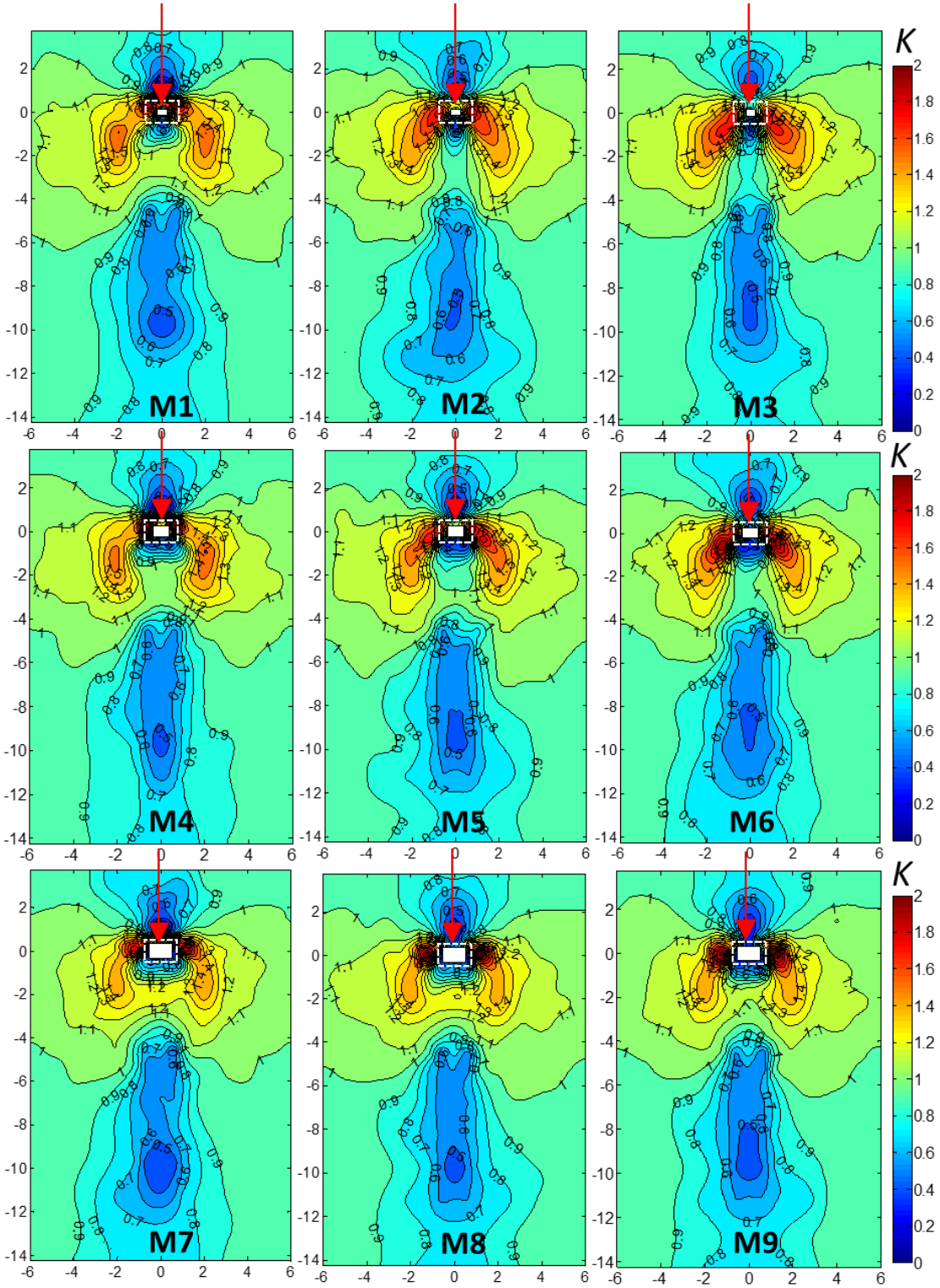

Figure 6. The distribution of the normalized mean wind speed ratio (*K*) in the surrounding of the 9 'lift-up' buildings

The observed flow modifications near the 'lift-up' buildings are qualitatively compared to the wind-tunnel test results corresponding to the control building (CB) by using the normalized difference of K values (ΔK) as defined in equation (4),

$$\Delta K = \frac{K_{M(x,y)} - K_{CB(x,y)}}{K_{CB(x,y)}} \quad (4)$$

In equation (4), $K_{M(x,y)}$ denotes the normalized wind speed ratio (K) at a location (x,y) in the surrounding of a 'lift-up' building, and $K_{CB(x,y)}$ denotes the K value at the same location but in the wind environment of the CB.

Figure 7 shows the distributions of the calculated ΔK values around the 9 'lift-up' buildings. The calculated ΔK values vary between +0.8 and -0.8, where each extreme value indicates significant differences between the pedestrian-level wind environments around a 'lift-up' building and the control building. Consequently, noticeable flow modifications are found at the locations where $\Delta K \geq 0.6$ or $\Delta K \leq -0.6$, and according to Figure 7, these modifications are largely localized around the building. A major portion of the surrounding areas of the 'lift-up' buildings has ΔK values higher than 0.6, especially at the lateral sides of the buildings. The higher ΔK values shown in Figure 7 suggest that 'lift-up' buildings tend to generate higher wind speeds at the pedestrian level than buildings without 'lift-up' floors. Compared to the extreme positive ΔK values, larger negative ΔK values ($\Delta K \leq -0.6$) in the upstream and downstream directions of buildings are varied considerably with the 'lift-up' core dimensions. For example, negative ΔK values are more pronounced on the leeward side of the smaller cores (e.g. AP=9%) than on the cores with larger areas such as AP=49%. Similarly, ΔK values in the upstream direction of the buildings depend on the 'lift-up' core dimensions such that smaller cores create larger positive ΔK values while larger cores are responsible for the negative ΔK

values. However, the ΔK values in the far field of the 'lift-up' buildings are insensitive to the 'lift-up' core dimensions as indicated by the small-valued ΔK (within the range of ±0.2).

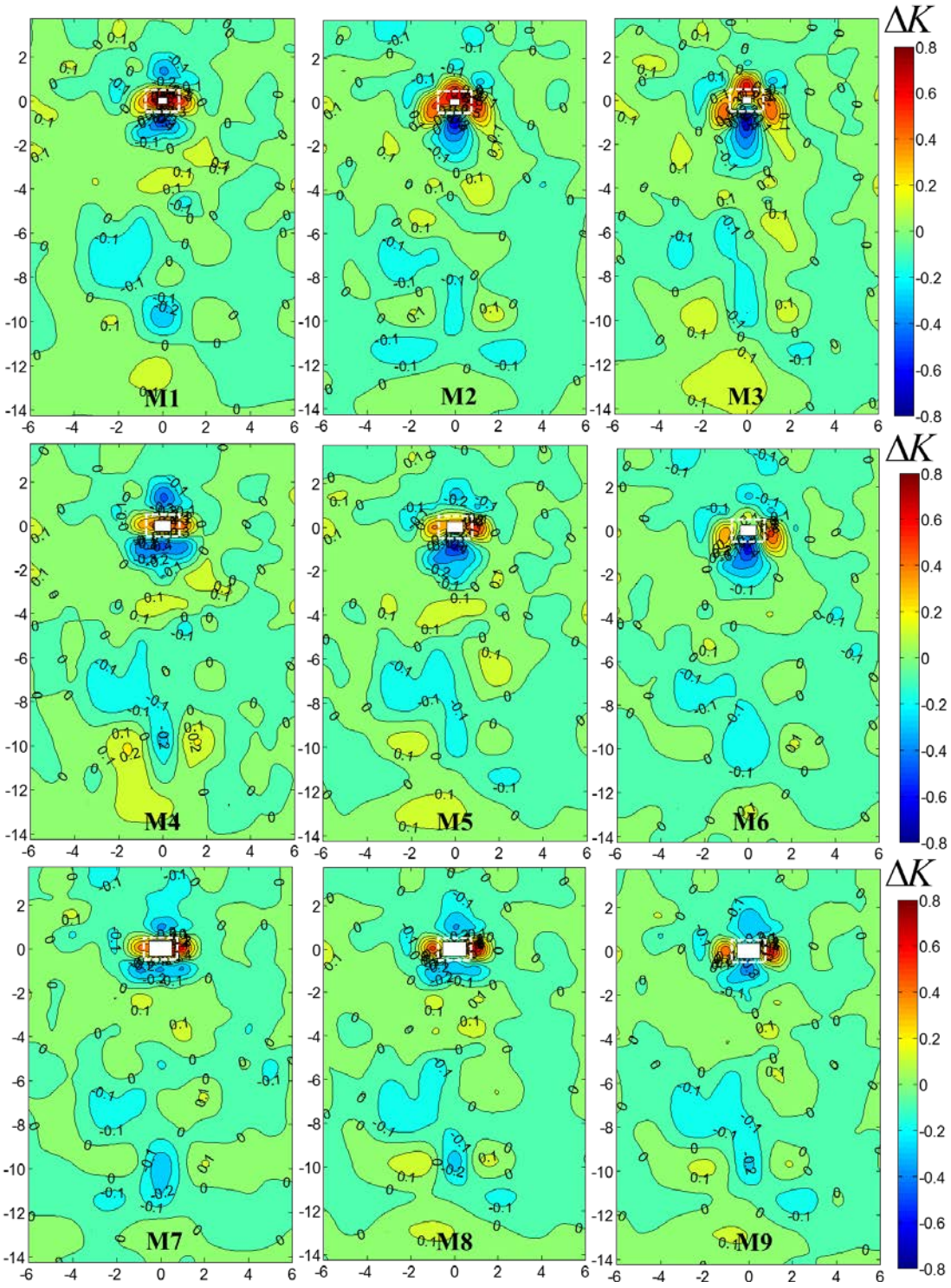

Figure 7. The distribution of the normalized difference of K values (ΔK) in the surrounding of the 9 'lift-up' buildings.

296 As is evident from Figures 6 and 7 the lift-up buildings modify their surrounding wind
297 environment differently than the building without 'lift-up' floors. The differences in the
298 pedestrian-level wind field around buildings with and without 'lift-up' designs are a result of
299 the formation of HWS and LWS zones and their variations in size and magnitude with the 'lift-
300 up' core dimensions. Therefore, the rest of the discussion focuses on examining the variations
301 of the HWS and LWS zones with the 'lift-up' core dimensions. Furthermore, the pedestrian-
302 level wind field in the 'lift-up' area is systematically investigated to show the characteristics
303 of the wind environment beneath the main structure of the 'lift-up' building.

304 *3.1.Variation of high wind speeds near the 'lift-up' area.*

305 Both the size and magnitude of the HWS zones vary with the 'lift-up' core dimensions as
306 shown in Figures 6 and 7. A new parameter, the area averaged high wind speed ratio ($\overline{K}_{HWS}$),
307 is introduced to estimate the general effect of the 'lift-up' core dimensions on the HWS zones
308 through a single value. It should be noted that only the areas with *K* values larger than 1.3 are
309 considered as HWS zones. According to this criterion, the $\overline{K}_{HWS}$ value is calculated as;

310 $$\overline{K}_{HWS} = \frac{\sum_{K=1.3}^{2} [A_{(K,K+0.1)} \times \overline{K}_{(K,K+0.1)}]}{A_{HWS}} \quad (5)$$

311 In equation (5), *K* is the contour level when the mean wind speed ratios are larger than 1.3,
312 A_{HWS} is the total area of the HWS zones, and $A_{(K,K+0.1)}$ is the area within the contour line between
313 *K* and *K+0.1*.

314 Figure 8 shows the calculated $\overline{K}_{HWS}$ values corresponding to the tested 'lift-up' building
315 models with different 'lift-up' core dimensions. The $\overline{K}_{HWS}$ value corresponding to the control
316 building (CB) is marked by a red dashed line in Figure 8 for the purpose of comparison. In
317 general, all the 'lift-up' buildings have larger $\overline{K}_{HWS}$ values than the control building ($\overline{K}_{HWS}$

=1.405) whereas the $\overline{K}_{HWS}$ values of the 'lift-up' buildings vary considerably with the 'lift-up' core height and area. In fact, the $\overline{K}_{HWS}$ values rapidly increase with the 'lift-up' height but decrease slightly with increasing core area. The increase of the $\overline{K}_{HWS}$ values with the core height is attributed to the accelerated wind flows in the 'lift-up' areas with taller cores where more space is available for the wind flow to pass through. On the other hand, significant wind blockage induced by shorter cores with larger areas, marginally reduces the $\overline{K}_{HWS}$ values. Therefore, an appropriate combination of core height and size would maximise the accelerated wind flows near 'lift-up' buildings as observed in model M6. The model M6, which has a taller core and a moderate core area (h=9m, AP=25%) has recorded the largest $\overline{K}_{HWS}$ value of 1.495 among all the tested 'lift-up' buildings in this study However, if the given objective of the design is to minimize the formation of HWS zones near 'lift-up' buildings, then the designer should select a short and bulky central core for the building such as in model M7.

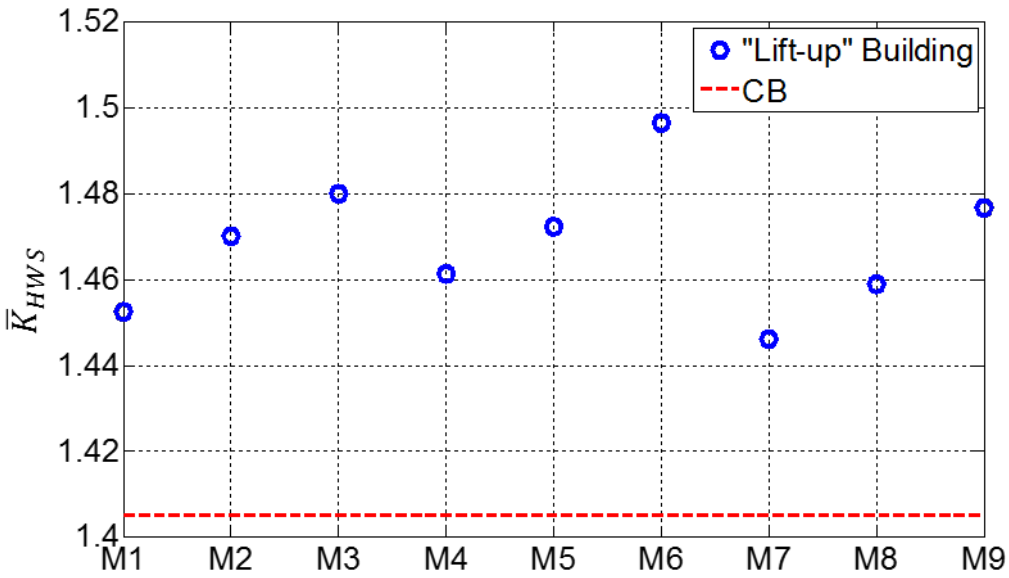

Figure 8. The area averaged high wind speeds ($\overline{K}_{HWS}$) near the 9 'lift-up' buildings and the control building (CB)

Although the overall influence of the 'lift-up' core dimensions on the HWS zone is indicated by the $\overline{K}_{HWS}$ value, it does not provide detailed information on the composition of the pedestrian-level wind speeds in the HWS zones created by 'lift-up' buildings. Consequently, the areas within the contours corresponding to different *K* values are employed to assess the composition of the wind speeds in the HWS zones. The area is then divided by the plan area of the building (*B* x *D*) to determine the normalized indicator: AP_{cum}. Figure 9 shows the variation of AP_{cum} with the corresponding *K* values for different building models. The variation of AP_{cum} corresponding to the control building (CB) is also included in Figure 9, as shown by the red solid line.

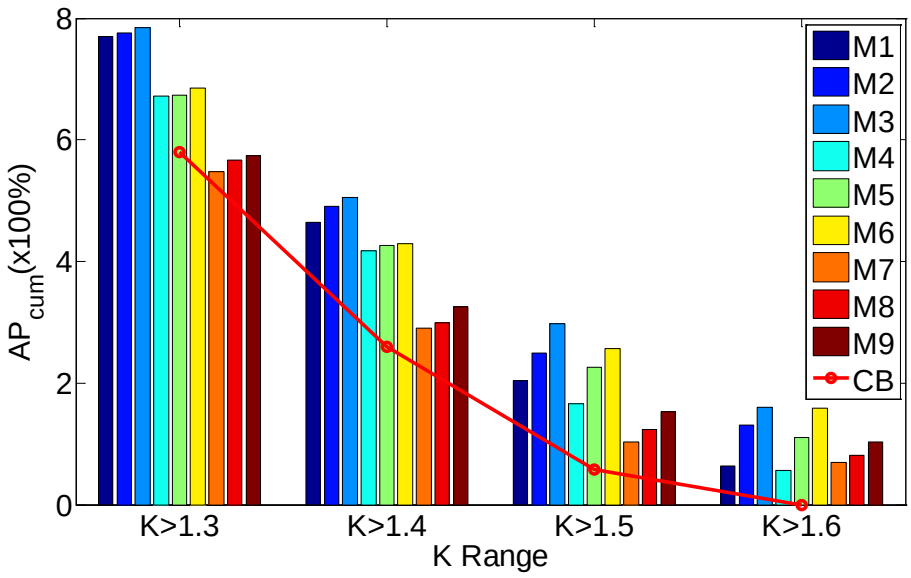

Figure 9. The distribution of normalised mean wind speed ratio (*K)* with the corresponding normalised area (AP_{cum}) for the 9 'lift-up' buildings and the control building (CB).

Figure 9 clearly shows that 'lift-up' buildings have higher wind speeds (e.g. *K*=1.5 and *K*=1.6) distributed over larger areas than the CB. In the case where the *K* value is higher than 1.6, all the 'lift-up' buildings generate AP_{cum} values larger than 0, whilst there is no measurable area of *K*>1.6 found for the CB. The variations of wind speeds and corresponding areas in the HWS zones in lift-up buildings are attributed to differences in core heights and areas of the 9 tested

buildings. For example, the influence of the 'lift-up' core height is more prominent at the higher end of the *K* values, such as *K*= 1.6, while core size governs the wind speeds and areas of the HWS zones at the lower end of *K* values in HWS (e.g. *K*<1.4).

3.2.Variation of low wind speeds near 'lift-up' buildings

Similar to the HWS zones, the influence of the 'lift-up' core dimensions on the low wind speed (LWS) zones is quantified using the area averaged low wind speed ratio ($\overline{K}_{LWS}$) as defined in equation (6). For the calculation, only areas with *K* values lower than 0.7 (*K*<0.7) are considered as LWS zones.

$$\overline{K}_{LWS} = \frac{\sum_{K=0}^{0.7} [A_{(\mathrm{K},\mathrm{K}+0.1)} \times \overline{K}_{(\mathrm{K},\mathrm{K}+0.1)}]}{A_{LWS}} \quad (6)$$

In equation.(6), *K* denotes the contour level corresponding to the mean wind speed ratios lower than 0.7; A_{LWS} is the total area of the LWS zones, and $A_{(K,K+0.1)}$ is the area within the contour lines between *K* and *K+0.1*.

In compliance with the selection criterion of the LWS zone, two distinct LWS zones are identified on the windward and leeward sides of the 'lift-up' buildings (Figure 6), and one noticeable LWS zone is observed upstream of the control building (Figure 5). To distinguish the variation of LWS in the upstream and downstream of buildings, the $\overline{K}_{LWS}$ values are separately calculated for the two directions in following subsections.

3.2.1. *Upstream Low Wind Speed (ULWS) zone*

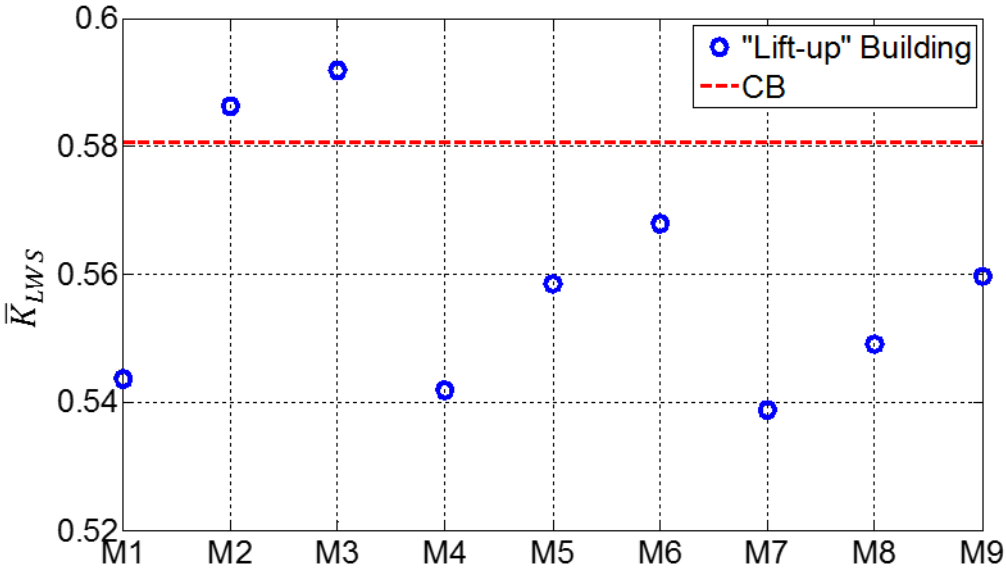

Figure 10. Area averaged low wind speeds ($\overline{K}_{LWS}$) in the ULWS zones of the 9 'lift-up' buildings and the control building (CB).

Figure 10 displays the calculated $\overline{K}_{LWS}$ values in the upstream low wind speed (ULWS) zones of the 'lift-up' buildings and the control building (red dash line). Except for models M2 and M3, $\overline{K}_{LWS}$ values in the ULWS zones of the 'lift-up' buildings are smaller than in the ULWS zones of the control building (CB). The higher $\overline{K}_{LWS}$ value of the CB than of 'lift-up' buildings is attributed to the difference between the LWS zones formed upstream of the 'lift-up' buildings and the CB. In general, there are two LWS zones formed upstream of the CB, which is a building without 'lift-up' design, one next to the windward side, and the other far upstream of the building (Tsang et al., 2012). However, the LWS zone far upstream is not visible for the CB in Figure 4(b) because it was formed outside the measurement area owing to the strong backflow. On the other hand, leakage of the downwash flow through the 'lift-up' area has weakened the backflow, and subsequently forms the second LWS zone in the far upstream of measurement area, as shown in Figure 6. It should be noted that the wind flow through the 'lift-up' area not only creates the second LWS zone but also controls the $\overline{K}_{LWS}$

values in the ULWS zones. Higher wind blockages induced by shorter cores with larger areas tend to stagnate more air on the windward side of the building and produced smaller $\overline{K}_{LWS}$ values as observed for model M7. 'Lift-up' buildings with taller cores with smaller *AP* values, on the other hand, produce higher $\overline{K}_{LWS}$ in the ULWS zone such as in the M2 and M3 cases. The 'lift-up' core height has a more influence on the $\overline{K}_{LWS}$ values in the ULWS zone than the core area, as shown in Figure 10. Figure 11 further substantiates the greater influence of the 'lift-up' core height on the *K* values and corresponding areas of the ULWS zone. Taller 'lift-up' cores reduce considerably the size of areas with lower *K* values and are sometimes able to eliminate undesirable low wind speeds completely in the upstream direction of a 'lift-up' building. No areas with $K<0.4$ found in the ULWS zone for model M3 is an example of the effectiveness of taller cores with smaller core areas to minimize stagnated air in the upstream of 'lift-up' buildings.

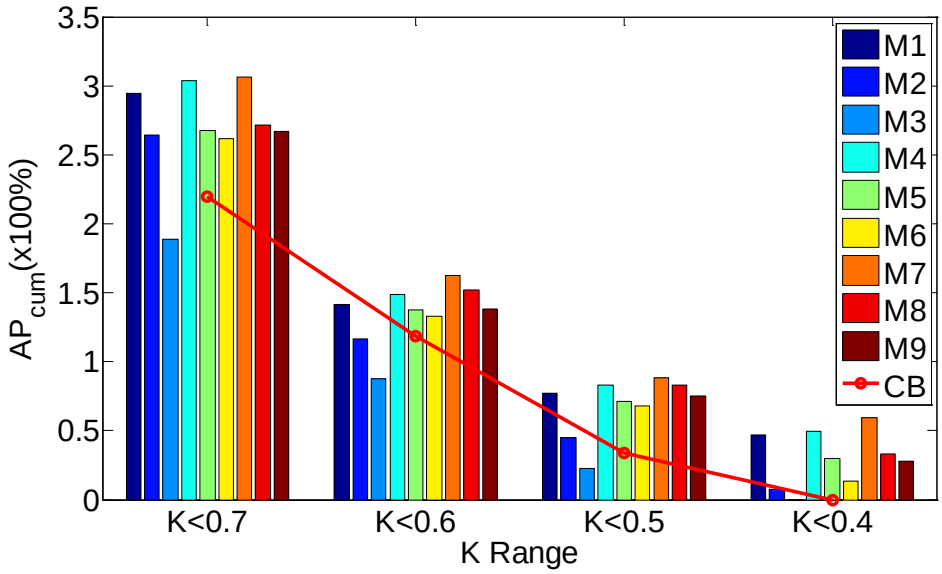

Figure 11. The distribution of normalised mean wind speed ratio (*K)* with the corresponding normalised area (AP_{cum}) of the ULWS zone for the 9 'lift-up' buildings and the control building (CB).

3.2.2. *Downstream Near-field Low Wind Speed (DNLWS) zone*

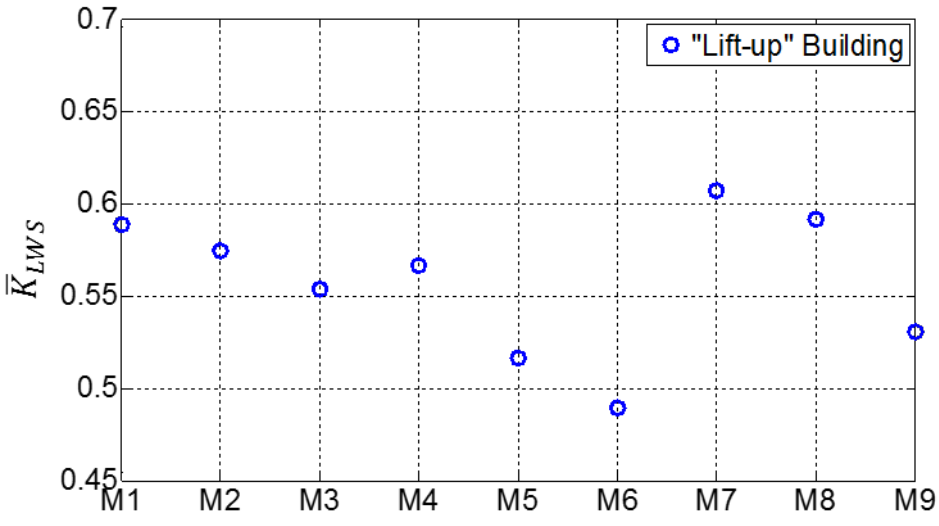

Figure 12. Area averaged low wind speeds ($\overline{K}_{LWS}$) in the DNLWS zone of the 9 'lift-up' buildings.

Figure 12 displays the $\overline{K}_{LWS}$ values in the DNLWS zone calculated only for the tested 9 lift-up buildings. The $\overline{K}_{LWS}$ value cannot be calculated for the control building (CB) as no LWS area (i.e., an area with K<0.7) is formed next to the leeward sides of the CB (Figure 5). The absence of DNLWS zone of the CB is attributed to the steady horseshoe vortex generated by the strong downwash along the front face of the CB. The steady horseshoe vortex of the CB wraps firmly around the base of the building and prevents the formation of a DNLWS zone on the leeward side of the CB (Tsang et al., 2012). The horseshoe vortices in each of the 'lift-up' buildings are, on the other hand, weaker because of the downwash flow passes through the 'lift-up' area. As a result, an LWS zone appear next to the leeward side of the 'lift-up' buildings, which have smaller $\overline{K}_{LWS}$ values than the $\overline{K}_{LWS}$ values obtained in the pedestrian-level wind field on the leeward side of the CB. In fact, the calculated $\overline{K}_{LWS}$ value of the CB is 0.85 and thus it does not appear in Figure 12, which has a set maximum $\overline{K}_{LWS}$ value of 0.7. In addition, Figure 12 reveals that the 'lift-up' core height further reduces the $\overline{K}_{LWS}$ values in the DNLWS

zone. It is reasonable to link the reduced $\overline{K}_{LWS}$ values to the increase of downwash passing through the taller 'lift-up' areas, which further weakens the horseshoe vortex generation.

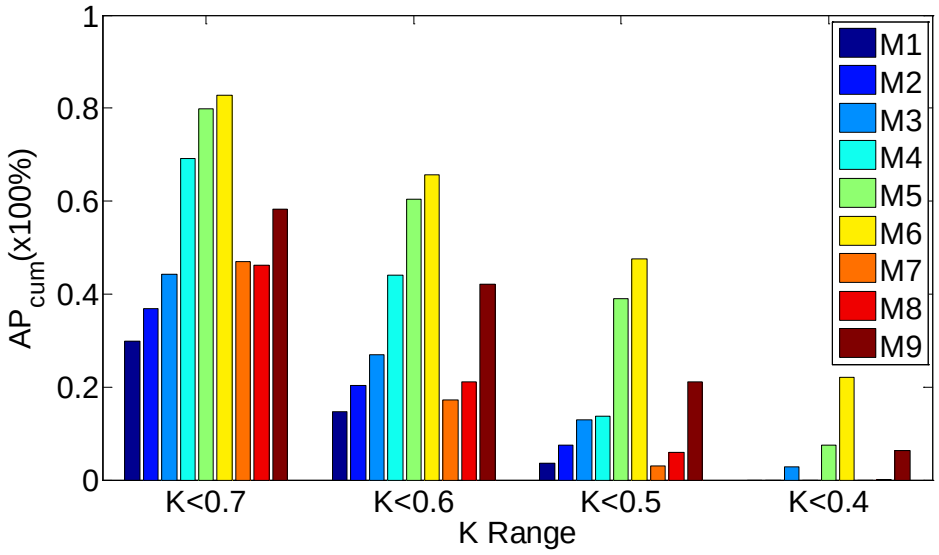

Figure 13. The distribution of normalised mean wind speed ratio (*K*) with the corresponding normalised area (AP_{cum}) of the DNLWS zone for the 9 'lift-up' buildings.

Figure 13 displays the variation of the area within a specific contour line (AP_{cum}) in the DNLWS zone with the corresponding *K* value. It should be noticed that Figure 13 does not show data related to the control building (CB) as its *K* values in the DNLWS are not less than 0.7. In other words, Figure 13 depicts that the most of 'lift-up' buildings, generally, corresponds to smaller *K* values (such as $K<0.4$) when comparing to higher *K* values ($K>0.7$) corresponding to the CB. Moreover, AP_{cum} values increase considerably with the 'lift-up' core height, especially when *K* values are smaller than 0.6. Furthermore, a distinct increasing trend of AP_{cum} is identified with the increase of 'lift-up' core area from the smallest (AP=9%) to moderate (AP=25%) values but such an increasing trend is interrupted as the core area increases from moderate to the largest (AP=49%). In fact, larger core areas (AP=49%) are linked to the smaller AP_{cum} value under the condition that $0.7<K<0.4$. The decrease of AP_{cum} with larger core areas may have resulted from the UNLWS zone shifted inside the 'lift-up' area rather than stretched

into the downstream direction of the building. Therefore, a part of the DNLWS zone within the 'lift-up' area is not counted in the calculation of AP_{cum} (see Figure 6). The inward expansion of the LWS zone is further analysed in the section focusing on the distribution of wind speeds in the 'lift-up' area.

3.3.Distribution of mean wind speed in the 'lift-up' area

Details of the distribution of pedestrian-level wind speeds in the 'lift-up' area are important in determining the comfort level and safety of people who use the 'lift-up' area for various purposes (see Figure 1). For example, high wind speeds in the 'lift-up' area may cause walking instabilities and ultimately cause to lose the body balance. Consequently, knowledge of the wind speed distributions in the 'lift-up' area provides the guidance for positioning the building entrances in order to prevent the high wind speed from worrying pedestrians. Low wind speeds, eventually lead to inadequate air ventilations to cause outdoor thermal discomfort of people in 'lift-up' areas. Moreover, the prevailing low wind speed could lead to accumulation of air pollutants in the 'lift-up' area, exposing people in lift-up areas to harmful health risks.

Figure 14 shows the distribution of K values in the 'lift-up' areas of the 9 'lift-up' building models to reveal the influence of the 'lift-up' core dimensions on the pedestrian-level wind field in the 'lift-up' area. For example, shorter cores with smaller core areas create larger high wind speed zones, which cover a major portion of the 'lift-up' area. On the other hand, low wind speeds prevail in the 'lift-up' areas corresponding to the cores with the largest area (AP=49%). Moreover, the cores with the smallest area (AP=9%) results in the low wind speed zone having a width approximately equal to the 'lift-up' core but in the 'lift-up' areas where the cores have larger areas (AP= 25% and 49%) then the low wind speed zone is wider than the cores. The low wind speed zones at the leeward side of the largest core (AP=49%), on the other hand, expand laterally rather than stretch downstream, which could explain the high $\overline{K}_{LWS}$ values and smaller AP_{cum} values corresponding to the buildings with the largest core, as

seen in Figures 12 and 13. The 'lift-up' core dimensions not only modify the pedestrian-level wind speed distribution but also define the location where the maximum and minimum wind speeds are observed. The maximum wind speeds in the 'lift-up' area of model M1 are found near the upstream corners of the building, while the maximum wind speeds in model M6 exist on the lateral sides of the core. In the extreme case, the location of the maximum wind speed may lie outside of the 'lift-up' area, as seen in the models M8 and M9, which have larger core areas.

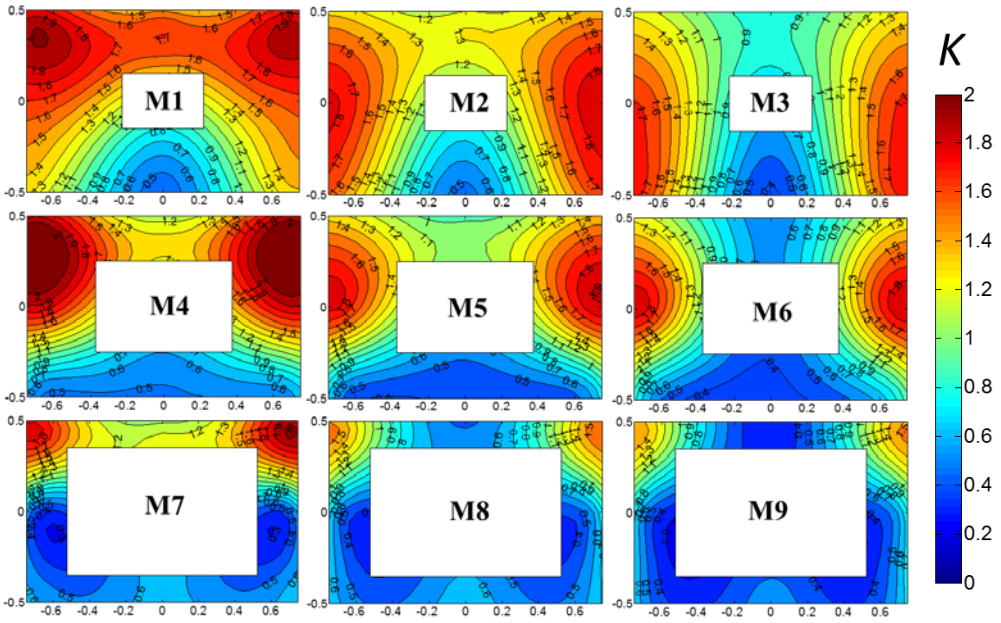

Figure 14. The distribution of normalised mean wind speed ratio (K) in the 'lift-up' areas of the 9 'lift-up' buildings (white rectangles represent the central core)

The distribution of pedestrian-level wind speeds in the 'lift-up' area can be employed to indicate appropriate 'lift-up' dimensions in terms of providing acceptable pedestrian-level wind conditions in the 'lift-up' area. The acceptable wind speeds at a given location depend on several factors such as the prevailing wind speed, air temperature, physical activities, and clothing (Lawson, 1978). Since the scope of the present study is limited to determining the effects of wind speeds on pedestrian comfort and safety, only a criterion based on the mean wind speed is presented to select appropriate 'lift-up' dimensions. The selected criterion

considers K values within the range of 0.7 to 1.3 as acceptable wind conditions by assuming K<0.7 indicates undesirable low wind speeds that cause the outdoor thermal discomfort and K>1.3 results in pedestrian discomfort due to high wind speeds. Since residential building sites usually have areas allocated for kids' playing areas, or sitting areas, the less perturbation concept, and hence the selected acceptable K value range, is reasonable and practical for the building design evaluation. However, the selected comfort criterion is arbitrary such as the criterion used by Uematsu et al., (1992) and only intends to demonstrate how to select appropriate lift-core dimensions based on a given comfort criterion. To achieve a higher accuracy in determining 'lift-up' core dimensions and to compatible with the prevailing wind conditions, it is advisable to employ a comprehensive comfort criterion together with meteorological data rather than a simple criterion similar used in the current study.

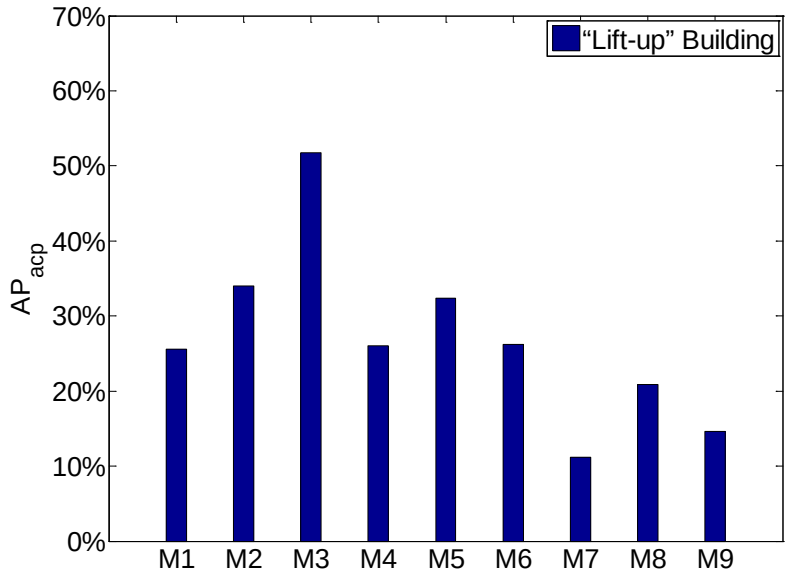

Figure 15. Area percentages of acceptable wind speeds (AP_{acp}) in the lift area of the 9 'lift-up' buildings

Figure 15 displays the percentages of the areas (AP_{acp}), which is the area with acceptable wind conditions normalized with respect to the usable plan area of the building (i.e., 1- AP) for the tested 9 'lift-up' buildings. As shown in Figure 15, model M3 has the most appropriate 'lift-up' dimensions to produce the largest area (AP_{acp} > 50%) with acceptable wind conditions (i.e.,

494 *K* values in the range of 0.7-1.3). In contrast, model M7, which has the shortest core with the
495 largest area (*h*=3m, *AP*= 49%) has the smallest area with acceptable wind conditions (AP_{acp}
496 =11%). Under the definition of acceptable wind conditions adopted in this study, the smallest
497 core (*AP*=9%) yields, in general, a better wind environment in the 'lift-up' area with AP_{acp}
498 values greater than 25%. The cores with larger areas, such as *AP*=25% and *AP*=49%, fall short
499 of achieving the acceptable pedestrian-level wind environment in the 'lift-up' area, and the
500 worst conditions are found for models M7, M8, and M9, which have the areas with acceptable
501 wind speeds less than 20% of the useable 'lift-up' area.

502 **4. Concluding remarks**

503 In the present study, the pedestrian-level wind fields around 'lift-up' buildings were
504 systematically investigated through a series of wind tunnel tests. The influence of the 'lift-up'
505 core dimensions was determined by testing 9 'lift-up' buildings with different 'lift-up' core
506 heights and core areas. The investigation used mean wind speeds measured at the 10mm height
507 (i.e., 2m height in full scale), and the normalized mean wind speed ratio (*K*) to analyse: (1) the
508 overall features of the pedestrian-level wind environment around the 'lift-up' buildings, (2) the
509 distribution of high and low wind speeds near the 'lift-up' buildings, and (3) the distribution of
510 wind speeds in the 'lift-up' area. Moreover, a control building of the same overall dimensions
511 but without a 'lift-up' core was tested using the same wind-tunnel setup, and the results were
512 compared to identify any wind conditions resulting from the 'lift-up' configuration. Based on
513 the wind tunnel test results, the following conclusions are drawn:

514 (1) A 'lift-up' building modifies its surrounding wind environment differently than a
515 building without 'lift-up' design (the control building) with similar dimensions. The
516 flow modifications include (1) increases in area and magnitude of high wind speed
517 (HWS) zones, (2) the formation of a pronounced low wind speed (LWS) zone on the
518 leeward side of the 'lift-up' building, and (3) a weakened LWS zone in the upstream

519 direction of the ‘lift-up’ building. All of these modifications are the direct results of the
520 wind flow that passes through the ‘lift-up’ area. Therefore, it is possible to maintain the
521 desired wind environment near a ‘lift-up’ building by controlling the amount of wind
522 flow passing through the ‘lift-up’ area or in other words, by adjusting the ‘lift-up’ core
523 dimensions.

524 (2) The area-averaged high wind speed ratio (the $\overline{K}_{HWS}$ value) of a ‘lift-up’ building is
525 considerably higher than of a building without ‘lift-up’ design due to the increases in
526 size and intensity of the HWS areas. The $\overline{K}_{HWS}$ value increases appreciably with the
527 increase of ‘lift-up’ core height and slightly decreases with the increase of the core area.
528 The effect of the ‘lift-up’ height is more pronounced for larger core areas (e.g.
529 *AP*=49%) than for smaller core areas such as *AP*=9%. Consequently, the ‘lift-up’ core
530 dimensions that consist of a moderate core area with the tallest core height (*AP*=25%,
531 *h*=9m) would result in the highest accelerated wind flows near a ‘lift-up’ building.

532 (3) The area averaged low wind speed ratio (the $\overline{K}_{LWS}$ value) of the two low wind speed
533 (LWS) zones around ‘lift-up’ buildings are smaller than the $\overline{K}_{HWS}$ value of a building
534 ‘lift-up’ design. Moreover, the core area has a greater influence on generating smaller
535 wind speeds in the upstream low wind speed (ULWS) zones than the ‘lift-up’ core
536 height. The ‘lift-up’ core height is effective in reducing the size of the ULWS areas of
537 ‘lift-up’ buildings with larger cores areas (e.g. *AP*=49%). The increase of both height
538 and area of the core decreases wind speeds in the downstream near-field low wind speed
539 (DNLWS) zone. However, $\overline{K}_{LWS}$ values in the DNLWS zone are slightly increased for
540 the largest core size of *AP*=49% due to the expansion of the LWS area from the leeward
541 side to the lateral sides of the core.

542 (4) Appropriate lift-up dimensions can be determined by combining a wide range of wind
543 speed data and meteorological wind data with a selection criterion, which depends on

the required wind conditions so as to increase or decrease the wind speeds near lift-up buildings. As the wind tunnel test results indicate that the ‘lift-up’ core height is the most influential parameter, the most appropriate ‘lift-up’ design can be determined by first selecting the core height and then choosing a suitable core area from examining the wind tunnel test data.

Acknowledgment

The work described in this paper was fully supported by a grant from the Research Grants Council of the Hong Kong Special Administrative Region, China (Project No. C5002-14G).The authors of this paper would like to express their gratitude to the staff of the Wind and Wave Tunnel Facility (WWTF) at the Hong Kong University of Science and Technology (HKUST) for their support during the wind tunnel experiments.

555 **References**

556 Beranek, W. J. (1984). Wind environment around single buildings of rectangular shape. Heron,
557 29(1), 3-31

558 Bottema, M. M. (1993). Wind climate and urban geometry (Doctoral dissertation, Technische
559 Universiteit Eindhoven).

560 Cheng, V., Ng, E., Chan, C., & Givoni, B. (2012). Outdoor thermal comfort study in a sub-
561 tropical climate: a longitudinal study based in Hong Kong. International journal of
562 biometeorology, 56(1), 43-56.

563 Chetwittayachan, T., Shimazaki, D., & Yamamoto, K. (2002). A comparison of temporal
564 variation of particle-bound polycyclic aromatic hydrocarbons (pPAHs) concentration
565 in different urban environments: Tokyo, Japan, and Bangkok, Thailand. Atmospheric
566 Environment, 36(12), 2027-2037.

567 Gandemer, J. (1975). Wind environment around buildings: aerodynamic concepts. In Proc., 4th
568 Int. Conf. Wind Effects on Buildings and Structures, Heathrow (pp. 423-432).

569 Goyal, P. (2002). Effect of winds on SO 2 and SPM concentrations in Delhi. Atmospheric
570 Environment, 36(17), 2925-2930.

571 Hang, J., & Li, Y. (2010). Ventilation strategy and air change rates in idealized high-rise
572 compact urban areas. Building and Environment, 45(12), 2754-2767.

573 Hosker, R. P. (1985). Flow around isolated structures and building clusters: a review. ASHRAE
574 Trans.;(United States), 91(CONF-850606-).

575 Irwin, H. P. A. (1981). A simple omnidirectional sensor for wind-tunnel studies of pedestrian-
576 level winds. Journal of Wind Engineering and Industrial Aerodynamics, 7(3), 219-239.

Jamieson, N. J., Carpenter, P., & Cenek, P. D. (1992). The effect of architectural detailing on pedestrian-level wind speeds. Journal of Wind Engineering and Industrial Aerodynamics, 44(1), 2301-2312.

Kawai, H. (1998). Effect of corner modifications on aeroelastic instabilities of tall buildings. Journal of Wind Engineering and Industrial Aerodynamics, 74, 719-729.

Lam, K. M. (1992). Wind environment around the base of a tall building with a permeable intermediate floor. Journal of Wind Engineering and Industrial Aerodynamics, 44(1-3), 2313-2314.

Lawson, T. V. (1978). The wind content of the built environment. Journal of Wind Engineering and Industrial Aerodynamics, 3(2-3), 93-105.

Melbourne, W. H., & Joubert, P. N. (1971). Problems of wind flow at the base of tall buildings. Proceedings Wind Effects on Buildings and Structures.

Murakami, S., Iwasa, Y., & Morikawa, Y. (1986). Study on acceptable criteria for assessing wind environment at ground level based on residents' diaries. Journal of Wind Engineering and Industrial Aerodynamics, 24(1), 1-18.

Ng, E. (2009). Policies and technical guidelines for urban planning of high-density cities–air ventilation assessment (AVA) of Hong Kong. Building and environment, 44(7), 1478-1488.

Stathopoulos, T., Wu, H., & Bédard, C. (1992). Wind environment around buildings: a knowledge-based approach. Journal of Wind Engineering and Industrial Aerodynamics, 44(1-3), 2377-2388.

Tamura, T., & Miyagi, T. (1999). The effect of turbulence on aerodynamic forces on a square cylinder with various corner shapes. Journal of Wind Engineering and Industrial Aerodynamics, 83(1), 135-145.

601 Tanaka, H., Tamura, Y., Ohtake, K., Nakai, M., & Kim, Y. C. (2012). Experimental
602 investigation of aerodynamic forces and wind pressures acting on tall buildings with
603 various unconventional configurations. Journal of Wind Engineering and Industrial
604 Aerodynamics, 107, 179-191.
605 Tsang, C. W., Kwok, K. C. S., & Hitchcock, P. A. (2012). Wind tunnel study of pedestrian-
606 level wind environment around tall buildings: Effects of building dimensions,
607 separation and podium. Building and environment, 49, 167-181.
608 Tse, K. T., Hitchcock, P. A., Kwok, K. C. S., Thepmongkorn, S., & Chan, C. M. (2009).
609 Economic perspectives of aerodynamic treatments of square tall buildings. Journal of
610 wind engineering and industrial aerodynamics, 97(9), 455-467.
611 Uematsu, Y., Yamada, M., Higashiyama, H., & Orimo, T. (1992). Effects of the corner shape
612 of high-rise buildings on the pedestrian-level wind environment with consideration for
613 mean and fluctuating wind speeds. Journal of Wind Engineering and Industrial
614 Aerodynamics, 44(1-3), 2289-2300.
615 Wang, X. K., & Lu, W. Z. (2006). Seasonal variation of air pollution index: Hong Kong case
616 study. Chemosphere, 63(8), 1261-1272.
617 Wu, H., & Stathopoulos, T. (1994). Further experiments on Irwin's surface wind sensor. Journal
618 of wind engineering and industrial aerodynamics, 53(3), 441-452.
619 Xia, Q., Liu, X., Niu, J., & Kwok, K. C. (2015). Effects of building lift-up design on the wind
620 environment for pedestrians. Indoor and Built Environment, 1420326X15609967.
621 Yim, S. H. L., Fung, J. C., Lau, A. K., & Kot, S. C. (2009). Air ventilation impacts of the “wall
622 effect” resulting from the alignment of high-rise buildings. Atmospheric environment,
623 43(32), 4982-4994.

624 Yu, I. T., Li, Y., Wong, T. W., Tam, W., Chan, A. T., Lee, J. H., Leung, D.Y.C., & Ho, T.
625 (2004). Evidence of airborne transmission of the severe acute respiratory syndrome
626 virus. New England Journal of Medicine, 350(17), 1731-1739.